Biophysical Journal, Volume 96

Supporting Material

A Novel Kinetic Assay of Mitochondrial ATP-ADP Exchange Rate Mediated by the ANT

Christos Chinopoulos, Szilvia Vajda, László Csanády, Miklós Mándi, Katalin Mathe, and Vera Adam-Vizi

The 'core' of the method for estimating ATP-ADP steady-state exchange rate lies in a reliable estimation of free [Mg^{2+}] in the range of 0.1-1 mM. Our calibration of MgG fluorescence (performed as detailed in "Materials and Methods") using Eq. M1 gave reasonable estimates of free [Mg^{2+}] ([Mg^{2+}]$_f$); in figure 1A, curve (a) shows the calibrated signal of MgG fluorescence upon adding 0.1 mM $MgCl_2$ boluses (arrows) to a solution initially devoid of Mg^{2+}. Because all Mg^{2+}-sensitive dyes also bind Ca^{2+} (MgG has a K_d=4.7 μM for Ca^{2+}), we tested the response of MgG fluorescence to consecutive boluses of 1 μM $CaCl_2$ (supplementary figure 1A, curve (b)). In the presence of 1 mM $MgCl_2$ MgG fluorescence, and hence the calculated free [Mg^{2+}] (curve (b)), was only marginally affected by boluses of $CaCl_2$. Note, that in our buffer the contaminating free [Ca^{2+}] is ~150 nM, as measured by fura-6F (K_d=2.47 μM (1), and fura 2 (K_d=0.225 μM in the presence of Mg^{2+}, not shown).

For the calculation of [ATP] from free [Mg^{2+}] (see Eq. 5, below), the apparent K_d values (at our pH of 7.25 and our temperature of 37°C) of Mg^{2+} for ADP and ATP are required. These can be calculated from the room-temperature values of the proton dissociation constants of ATP (or ADP) and the association constants of ATP^{4-} and $ATPH^{3-}$ (or ADP^{3-} and $ADPH^{2-}$) for Mg^{2+}, by taking into account the dependencies of these parameters on temperature – all these parameters have been estimated previously by others (4-6). However, differing values have been reported for these constants in different studies, while our calculation of [ATP] from free [Mg^{2+}] (Eq. 5) is non-linear in nature, and even small differences in K_d could result in large errors in [ATP] estimates. Therefore, we directly determined the apparent K_d of Mg^{2+} for ADP (K_{ADP}) and for ATP (K_{ATP}) under our conditions by stepwise titration of Mg^{2+} with the respective nucleotide (supplementary figure 1B, C). ADP and ATP were added in 0.25 mM and 0.2 mM boluses, respectively, to a medium containing a total concentration of 1 mM Mg^{2+} and the free [Mg^{2+}] was measured using MgG. To obtain K_d values, free [Mg^{2+}] versus total [nucleotide] plots (supplementary Fig. 1B,C; *dots*) were fitted by least squares (supplementary Fig. 1B,C; *solid lines*) to the binding equation

$$[Mg^{2+}]_f = 0.5 \cdot \left([Mg^{2+}]_t - K_d - [L]_t + \sqrt{\left([Mg^{2+}]_t - K_d - [L]_t\right)^2 + 4K_d[Mg^{2+}]_t} \right), \qquad \text{(Eq. 2)}$$

where [Mg^{2+}]$_t$ is the total [Mg^{2+}] (1 mM), $[L]_t$ is the total concentration of added ADP or ATP, and K_d is the fitted value of K_{ADP} or K_{ATP}, respectively. From our fits we obtained estimates of K_{ADP}=0.906 ± 0.023 mM (supplementary Fig. 1B), and K_{ATP}=0.114 ± 0.005 mM (supplementary Fig. 1C). As a comparison, the program Winmaxc (http://www.stanford.edu/~cpatton/maxc.html), using Martell and Smith's and Fabiato A. and Fabiato F.'s constants (2) predicts apparent K_d values of K_{ADP}=0.739 mM, and K_{ATP}=0.060 mM – in reasonable agreement with our measured values.

Evaluation of ATP-ADP steady-state exchange rate by calculating the total [ATP] released from measured free extramitochondrial [Mg^{2+}]

Addition of 2 mM ADP to a medium containing mitochondria, AP_5A, substrates, 1 mM $MgCl_2$, and 2 μM MgG causes an immediate drop in free [Mg^{2+}], from 1 mM to ~0.39 mM (figure 1A of the manuscript), which is in agreement with the calculated value (0.3939 mM) considering the K_{ADP} value estimated above (supplementary figure 1B and Eq. 2). Under these conditions oxidative phosphorylation is initiated and for the next 25 sec is maintained, while ADP is replaced in the medium with ATP. Because ATP binds Mg^{2+} with a higher affinity than does ADP, this process is reflected by a further gradual decline in the free [Mg^{2+}] (figure 1A of the

manuscript). Addition of 4 μM cATR, a specific inhibitor of ANT, immediately stops this progressive decrease in free $[Mg^{2+}]$(figure 1A of the manuscript), consistent with the fact that under these conditions the ANT is the sole mediator of ADP/ATP exchange. cATR binds to ANT with a very high affinity (K_d=10^{-8} M); because this binding is non-competitive (unlike for atractyloside), ADP even in high concentrations cannot overcome the inhibition (8). Since one molecule of cATR binds to one ANT dimer, and mitochondrial preparations contain 0.24-1.8 nmol of ANT per mg protein (depending on the tissue; (3, 7) plus our own estimates, see below), 4 μM cATR is sufficient to inhibit all molecules of ANT in our mitochondrial suspension (1 mg of mitochondrial protein per 2 ml). Free $[Mg^{2+}]$ also ceased to decline upon addition of 10 μM oligomycin (not shown). Including the adenylate kinase inhibitor AP_5A into the medium is essential; Mg^{2+}, which is present in the assay medium, activates adenylate kinase http://www.brenda-enzymes.info/php/result_flat.php4?ecno=2.7.4.3) which exhibits an appreciable activity in some tissues. Significant production of ATP by this enzyme, upon addition of 2 mM ADP, would result in overestimation of ATP-ADP steady-state exchange rate mediated by the ANT. When AP_5A was omitted from the medium, we indeed observed a faster decrease in free $[Mg^{2+}]$ upon ADP addition and free $[Mg^{2+}]$ continued to fall (although at a lower rate) even after addition of cATR (not shown).

To convert measured $[Mg^{2+}]_f$ into total [ATP] in the medium ($[ATP]_t$), we assumed that in our medium the system

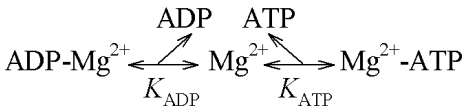

is at equilibrium at any moment. This is a fair assumption, as the rate of Mg^{2+} binding to, and unbinding from, nucleotides is faster than the rate of ATP/ADP exchange across mitochondrial membranes (diffusion of ions in solution is several orders of magnitude faster than any conformational transitions of proteins). Thus, at any moment, $[Mg^{2+}]_t$ in the medium is distributed between three equilibrium pools, free, ADP-bound, and ATP-bound:

$$[Mg^{2+}]_t = [Mg^{2+}]_f + \frac{[Mg^{2+}]_f[ADP]_t}{K_{ADP} + [Mg^{2+}]_f} + \frac{[Mg^{2+}]_f[ATP]_t}{K_{ATP} + [Mg^{2+}]_f}, \quad \text{(Eq. 3)}$$

where $[ADP]_t$ and $[ATP]_t$ are the total concentrations of ADP and ATP, respectively, in the medium.

Because the ANT exchanges ADP for ATP at a 1:1 stoichiometry, $[ADP]_t$+$[ATP]_t$ remains constant in the extramitochondrial compartment throughout the experiment. In particular, at any time point

$$[ADP]_t = [ADP]_t(t=0) + [ATP]_t(t=0) - [ATP]_t, \quad \text{(Eq. 4)}$$

where $[ADP]_t(t=0)$ and $[ATP]_t(t=0)$ are $[ADP]_t$ and $[ATP]_t$ in the medium at time zero (2 mM and 0 mM, respectively – our ADP stock solution exhibited negligible contamination with ATP). Substituting $[ADP]_t$ from the latter equation into Eq. 3, and rearranging Eq. 3 to express $[ATP]_t$ we get

$$[ATP]_t = \left(\frac{[Mg^{2+}]_t}{[Mg^{2+}]_f} - 1 - \frac{[ADP]_t(t=0) + [ATP]_t(t=0)}{K_{ADP} + [Mg^{2+}]_f} \right) \Bigg/ \left(\frac{1}{K_{ATP} + [Mg^{2+}]_f} - \frac{1}{K_{ADP} + [Mg^{2+}]_f} \right) \quad \text{(Eq. 5).}$$

Equation 5 is available for download as an executable file at http://www.oxphos.com/index.php?option=com_remository&Itemid=40&func=select&id=9, or from the supplementary material. To verify the reliability of the $[ATP]_t$ estimates obtained using Eq. 5 and measured values of $[Mg^{2+}]_f$, we applied the above algorithm to a series of solutions with known $[ATP]_t$ (Fig. 1D). To this end, 0.1 mM ATP boluses were added in a stepwise fashion to a 2-ml aliquot of our bath solution containing 2 mM ADP and MgG. After each ATP bolus $[Mg^{2+}]_f$ was determined from MgG fluorescence using Eq. 2; and [ATP]t was estimated using Eq. 5 in which $[ADP]_t(t=0)+[ATP]_t(t=0)$ was set to 2 mM+*i**0.1 mM (*i*=1, 2, ...7) for the trial following the *i*th ATP bolus. A plot of calculated $[ATP]_t$ values as a function of true $[ATP]_t$ for this series of experiments (supplementary Fig. 1D) convinced us that we could predict $[ATP]_t$ in the medium with reasonable accuracy.

Reference List

1. Chinopoulos, C., A. A. Starkov, and G. Fiskum. 2003. Cyclosporin A-insensitive permeability transition in brain mitochondria: inhibition by 2-aminoethoxydiphenyl borate. *J. Biol. Chem.* 278:27382-27389.

2. Fabiato, A. and F. Fabiato. 1979. Calculator programs for computing the composition of the solutions containing multiple metals and ligands used for experiments in skinned muscle cells. *J. Physiol (Paris)* 75:463-505.

3. Forman, N. G. and D. F. Wilson. 1983. Dependence of mitochondrial oxidative phosphorylation on activity of the adenine nucleotide translocase. *J. Biol. Chem.* 258:8649-8655.

4. Martell, A. E. and R. M. Smith. 1974. Critical Stability Constants. Plenum Press, New York.

5. Phillips, R. C., P. George, and R. J. Rutman. 1963. POTENTIOMETRIC STUDIES OF THE SECONDARY PHOSPHATE IONIZATIONS OF AMP, ADP, AND ATP, AND CALCULATIONS OF THERMODYNAMIC DATA FOR THE HYDROLYSIS REACTIONS. *Biochemistry* 2:501-508.

6. Phillips, R. C., P. George, and R. J. Rutman. 1966. Thermodynamic studies of the formation and ionization of the magnesium(II) complexes of ADP and ATP over the pH range 5 to 9. *J. Am. Chem. Soc.* 88:2631-2640.

7. Rossignol, R., T. Letellier, M. Malgat, C. Rocher, and J. P. Mazat. 2000. Tissue variation in the control of oxidative phosphorylation: implication for mitochondrial diseases. *Biochem. J.* 347 Pt 1:45-53.

8. Vignais, P. V., P. M. Vignais, and G. Defaye. 1971. Gummiferin, an inhibitor of the adenine-nucleotide translocation. Study of its binding properties to mitochondria. *FEBS Lett.* 17:281-288.

Legend to Supplementary figure 1: Dependence of MgG fluorescence on $[Mg^{2+}]_f$ and $[Ca^{2+}]_f$ and determination of K_d for Mg-AdNucl complexes. A: Reconstructed time courses of free $[Mg^{2+}]$, calculated from MgG fluorescence using Eq.2. In curve '**a**', 0.1 mM $MgCl_2$ boluses were added, where indicated (*arrows*), to a 2-ml medium (see Materials and Methods for composition) initially devoid of Mg^{2+}, containing 2 μM MgG $5K^+$ salt. In curve '**b**', 1 mM $MgCl_2$ was already present in the medium at the onset, and 1 μM $CaCl_2$ boluses were added where indicated (*arrows*). **B**: Determination of K_d of ADP for Mg^{2+} by sequential addition of 18 boluses of ADP (0.25 mM each) while recording MgG fluorescence. Dots illustrate calculated free $[Mg^{2+}]$ after each bolus. The solid line is a fit to Eq.2, yielding the K_d value shown. **C**: Determination of K_d of ATP for Mg^{2+} by sequential addition of 10 ATP boluses (0.2 mM each). Details are as in B. All panels (A, B, C) share the same y-axis, i.e. $[Mg^{2+}]_f$ (mM). **D**: Plot of calculated $[ATP]_t$ values as a function of true $[ATP]_t$.

Legend to Supplementary figure 2: Dependence of MgG fluorescence on $[Mg^{2+}]_f$ in the presence of 1 mM ADP, mitochondria and cATR. **A**: Raw MgG fluorescence as a function of time. 0.1 mM MgCl2 boluses were added to a 2-ml medium (see Materials and Methods for composition) initially devoid of Mg^{2+}, containing 2 μM MgG $5K^+$ salt. **B**: Conversion of MgG fluorescence shown in panel A to $[Mg^{2+}]_f$, in the 0.1-2.5 mM range using a calibration curve as described in the Materials and Methods. The inset of panel B shows a linear regression of the first 6 additions of $MgCl_2$ of the same calibration curve.